

Phase-sensitive detection of dipole radiation in a fiber-based high numerical aperture optical system

A. N. Vamivakas, S. B. Ippolito, A. K. Swan, and M. S. Ünlü

Department of Electrical and Computer Engineering, Boston University, Boston, Massachusetts 02215, USA

M. Dogan, E. R. Behringer, and B. B. Goldberg

Department of Physics, Boston University, Boston, Massachusetts 02215, USA

Received September 20, 2006; revised December 29, 2006; accepted January 4, 2007;
posted January 22, 2007 (Doc. ID 74869); published March 19, 2007

We theoretically study the problem of detecting dipole radiation in a fiber-based confocal microscope of high numerical aperture. By using a single-mode fiber, in contrast to a hard-stop pinhole aperture, the detector becomes sensitive to the phase of the field amplitude. We find that the maximum in collection efficiency of the dipole radiation does not coincide with the optimum resolution for the light-gathering instrument. The derived expressions are important for analyzing fiber-based confocal microscope performance in fluorescence and spectroscopic studies of single molecules and/or quantum dots. © 2007 Optical Society of America
OCIS codes: 180.1790, 260.1960, 260.2110, 300.6280.

The confocal microscope is a ubiquitous tool for the optical study and characterization of single nanoscale objects. The rejection of stray light from the optical detector afforded by the confocal microscope, combined with its three-dimensional resolution, makes it an ideal instrument for studying physical systems with weak light emission properties.^{1,2} The electromagnetic dipole is the canonical choice for modeling the radiative properties of most physical systems. And, although the vector-field image of an electromagnetic dipole in a high numerical aperture confocal microscope has been known for some time,³ only recently have the light-gathering properties of the instrument been studied. Specifically, the collection-efficiency function for a confocal microscope based on a hard-stop aperture was defined and studied by Enderlein⁴ and was found to be sensitive to field intensity.

Confocal microscopes based instead on optical fiber apertures have also been investigated. The image-forming properties of both coherent⁵ and incoherent⁶ fiber-based confocal microscopes, as well as the light-gathering properties⁷ of the microscope with a reflecting object, have all been examined assuming the paraxial approximation to scalar diffraction theory. Since high numerical aperture fiber-based confocal microscopes are routinely employed in the study of silicon integrated circuits,⁸ single semiconductor quantum dots,⁹ and other nanoscale light emitters,¹⁰ it is of great practical interest to understand the light collection properties of the fiber-based instrument. Here, we extend the previous studies by using the angular spectrum representation^{1,11,12} (ASR) to study the coupling of dipole radiation into a single-mode optical fiber where we find, in contrast to the hard-stop aperture, efficient detection of dipole radiation requires mode matching the dipole image field to the fiber spatial mode profile.

For the calculation below, we assume the optical system illustrated in Fig. 1 is aplanatic. In what fol-

lows, we refer to reference sphere 1 as the collection objective and reference sphere 2 as the focusing objective. Initially, we assume the dipole $\vec{\mathbf{d}}$ is placed at the Gaussian focus of the collection objective. The cylindrical optical fiber facet is coaxial with the optical system axis (in Fig. 1), and its flat face is parallel to the focal plane of the focusing objective. We define the relevant angles, unit vectors, and wave vectors in Fig. 1. The sine condition relates the polar angles in the object and image space as $f_1 \sin \theta_1 = f_3 \sin \theta_3$, where we have introduced the focal length $f_1(f_3)$ for the collection (focusing) objective. To calculate the vector-wave-optics image of the dipole, we employ the ASR and express the image dipole field as

$$\begin{aligned} \vec{\mathbf{E}}_3(\vec{\mathbf{r}}_3) = & \frac{\tilde{M}^2 C}{\pi} \int_0^{\theta_3^{\max}} \int_0^{2\pi} d\theta_3 d\phi_3 \sqrt{\frac{\cos \theta_3}{\cos \theta_1}} \sin \theta_3 \\ & \times \{-\hat{\mathbf{n}}_{\theta_3}[\hat{\mathbf{n}}_{\theta_3} \cdot \vec{\mathbf{E}}_d] - \hat{\mathbf{n}}_{\phi_3}[\hat{\mathbf{n}}_{\phi_3} \cdot \vec{\mathbf{E}}_d]\} e^{i\vec{\mathbf{k}}_3 \cdot \vec{\mathbf{r}}_3}, \end{aligned} \quad (1)$$

where the focal length ratio $\tilde{M} = (f_3/f_1)$ (the optical system magnification $M = \tilde{M}n_1/n_3$), $C = ik_0^3(n_1n_3)^{1/2} \exp(if_1[k_1 - k_3\tilde{M}]) / (8\pi\tilde{M}\epsilon_0)$, and we integrate over the polar angle θ_3 and the azimuthal angle ϕ_3 in the image space. To arrive at Eq. (1), we map the vector electric far field of the dipole, $\vec{\mathbf{E}}_d$, across the collection objective and then across the focusing objective according to the unit vector mappings defined in Fig. 1. We find it convenient to integrate over the object space polar angle. Introducing the identity $d\theta_3 \sin \theta_3 = (\sin \theta_1 \cos \theta_1 / \tilde{M}^2 \cos \theta_3) d\theta_1$ into Eq. (1) and using Bessel function identities¹ to integrate over the azimuthal angle ϕ_3 we find

$$\begin{aligned}\vec{\mathbf{E}}_3^x(\vec{\mathbf{r}}_3) &= Cd_x \begin{bmatrix} \tilde{I}_{d0} + \tilde{I}_{d2} \cos 2\varphi_3 \\ \tilde{I}_{d2} \sin 2\varphi_3 \\ -2i\tilde{I}_{d1,2} \cos \varphi_3 \end{bmatrix}, \\ \vec{\mathbf{E}}_3^y(\vec{\mathbf{r}}_3) &= Cd_y \begin{bmatrix} \tilde{I}_{d2} \sin 2\varphi_3 \\ \tilde{I}_{d0} - \tilde{I}_{d2} \cos 2\varphi_3 \\ -2i\tilde{I}_{d1,2} \sin \varphi_3 \end{bmatrix}, \\ \vec{\mathbf{E}}_3^z(\vec{\mathbf{r}}_3) &= Cd_z \begin{bmatrix} 2i\tilde{I}_{d1} \cos \varphi_3 \\ 2i\tilde{I}_{d1} \sin \varphi_3 \\ -2\tilde{I}_{d0,2} \end{bmatrix},\end{aligned}\quad (2)$$

where we use the notation $\vec{\mathbf{E}}_3^j(\vec{\mathbf{r}}_3)$ for the image field of a j -oriented dipole in the object space expressed in terms of Cartesian unit vectors. The integrals \tilde{I}_{dn} are defined as

$$\tilde{I}_{d0} = \int_0^{\theta_1^{\max}} d\theta_1 f(\theta_1) (1 + \cos \theta_1 g(\theta_1)) J_0,$$

$$\tilde{I}_{d1} = \int_0^{\theta_1^{\max}} d\theta_1 f(\theta_1) g(\theta_1) \sin \theta_1 J_1,$$

$$\tilde{I}_{d2} = \int_0^{\theta_1^{\max}} d\theta_1 f(\theta_1) (1 - \cos \theta_1 g(\theta_1)) J_2,$$

$$\tilde{I}_{d0,2} = \int_0^{\theta_1^{\max}} d\theta_1 f(\theta_1) \sin^2 \theta_1 \tilde{M}^{-2} J_0,$$

and

$$\tilde{I}_{d1,2} = \int_0^{\theta_1^{\max}} d\theta_1 f(\theta_1) \cos \theta_1 \sin \theta_1 \tilde{M}^{-2} J_1, \quad (3)$$

where $f(\theta_1) = e^{ik_3 z_3 g(\theta_1)} (\cos \theta_1 / g(\theta_1))^{1/2} \sin \theta_1$, $g(\theta_1) = (1 - (\sin \theta_1 / \tilde{M})^2)^{1/2}$, the numerical aperture (NA_1) in the object space defines θ_1^{\max} as $\text{NA}_1 = n_1 \sin \theta_1^{\max}$, and J_m are order $m=0,1,2$ ordinary Bessel functions with argument $(k_3 \rho_3 / \tilde{M}) \sin \theta_1$. Equations (2) and (3) assume the dipole is situated at the Gaussian focus of the collection objective. To express the image of a displaced dipole located at (ρ_o, ϕ_o, z_o) , we use the imaging property of the optical system and introduce $\rho_{\text{new}} = \rho_3 + M\rho_o$, $\varphi_3 = \varphi_o$ and $z_{\text{new}} = z_3 + z_o M^2 (n_3/n_1)$ into Eqs. (2) and (3), where M is the optical system magnification.

We model the case when the phase-sensitive detector of the dipole field is a single-mode cylindrical optical fiber situated in the image space of the optical system. We define the collection efficiency $\eta(\vec{\mathbf{r}}_o; \tilde{M})$ of the optical fiber as

$$\eta(\vec{\mathbf{r}}_o; \tilde{M}) = \frac{\left| \int \vec{\mathbf{E}}_3^*(\vec{\mathbf{r}}_3; \vec{\mathbf{r}}_o) \cdot \vec{\mathbf{E}}_{\text{lm}}^j(\vec{\mathbf{r}}_3) dA_3 \right|^2}{\int |\vec{\mathbf{E}}_3(\vec{\mathbf{r}}_3; \vec{\mathbf{r}}_o = 0)|^2 dA_3 \int |\vec{\mathbf{E}}_{\text{lm}}^j(\vec{\mathbf{r}}_3)|^2 dA_3}, \quad (4)$$

where we make explicit the dependence of $\eta(\vec{\mathbf{r}}_o; \tilde{M})$ on the dipole location $\vec{\mathbf{r}}_o$ in the object space, and on the objective focal length ratio \tilde{M} of the optical system illustrated in Fig. 1. We point out that the collection efficiency, as defined in Eq. (4), depends on the overlap of the dipole image field amplitude with the fiber mode profile and not on the intensity of the dipole image field. For the single-mode optical fiber, with core radius a , we make the weakly guiding approximation,¹³ which results in the following normalized electric-field solutions¹⁴:

$$\vec{\mathbf{E}}_{01}^x(\vec{\mathbf{r}}, t) = \begin{cases} NJ_0\left(\frac{ur}{a}\right) e^{i\beta z} \hat{\mathbf{n}}_x & r \leq a \\ N \frac{J_0(u)}{K_0(w)} K_0\left(\frac{wr}{a}\right) e^{i\beta z} \hat{\mathbf{n}}_x & r \geq a \end{cases}, \quad (5)$$

where N is a normalization constant, $u = a\sqrt{n_{\text{co}}^2 k_o^2 - \beta^2}$ and $w = a\sqrt{\beta^2 - n_{\text{cl}}^2 k_o^2}$ are the transverse wavenumbers in the fiber core and cladding, $V^2 = u^2 + w^2 = ak_o\sqrt{n_{\text{co}}^2 - n_{\text{cl}}^2}$ is the fiber V -parameter, K_l is the order l modified Bessel function of the second kind, and the solution for the orthogonally polarized solution is obtained by interchanging x with y in Eq. (5).

We now apply the previous formalism, defining all relevant system parameters in the last line of the caption to Fig. 2, to study the collection efficiency of a fiber-based confocal microscope. First, we position the dipole in the focus (at the coordinate origin) of the collection objective and calculate the collection effi-

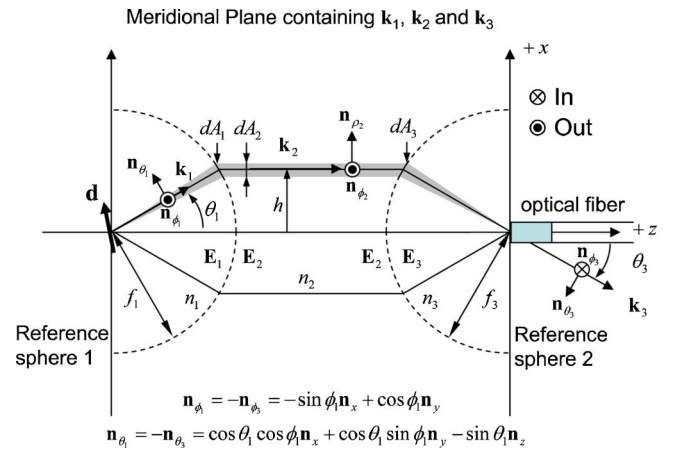


Fig. 1. (Color online) Optical system geometry used to image an arbitrarily oriented dipole $\vec{\mathbf{d}}$. The phase-sensitive detector, an optical fiber, is situated in the image space of the microscope. In each section of the optical system the magnitude of the wavevector relates to $|\mathbf{k}_0| = \omega/c$ as $|\mathbf{k}_i| = n_i |\mathbf{k}_0|$, where n_i is the refractive index.

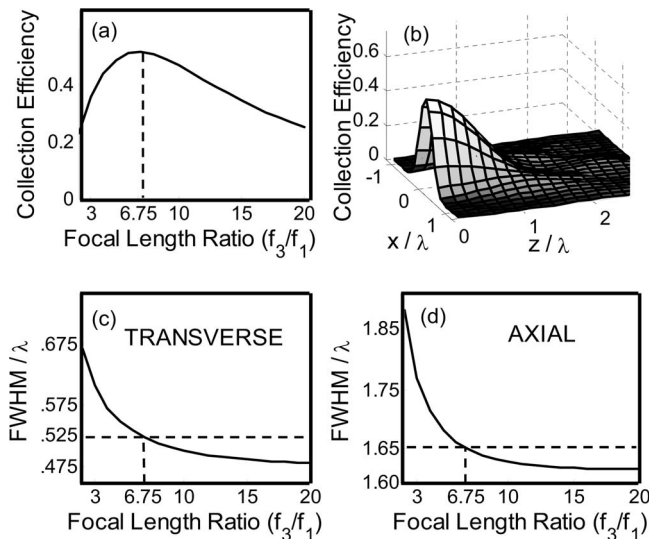


Fig. 2. (a) Collection efficiency $\eta(x_o=0, y_o=0, z_o=0; \tilde{M}=f_3/f_1)$ for a dipole situated at the object space origin. The dashed vertical line indicates the collection-efficiency maximum at $\tilde{M}=6.75$. (b) Collection efficiency $\eta(x_o=x, y_o=0, z_o=z; \tilde{M}=6.75)$, at the focal length ratio of maximum collection determined in (a), as the dipole is displaced in the object space of the microscope. (c) [(d)] The transverse (axial) resolution, quantified with the Houston criteria, for the linecut $\eta(x_o=x, z_o=0; \tilde{M})$ [$\eta(x_o=0, z_o=z; \tilde{M})$] as a function of $\tilde{M}=f_3/f_1$. In both (c) and (d), the dashed vertical line is at the focal length ratio of maximum collection efficiency [as determined from (a)]. (c) and (d) make clear the focal length ratio of maximum collection efficiency does not coincide with the focal length ratio of optimal resolution (minimum of the FWHM). For (a)–(d), in evaluating the collection efficiency, we average a uniform distribution of dipole orientations in the object space and assume $n_1=1.33$, $n_3=1$, $a=0.5\lambda$, $V=1.03$, and the collection objective NA₁ = 1.2.

ciency $\eta(\vec{r}_o=0; \tilde{M})$, averaged over a uniform distribution of dipole orientations in the object space, as a function of \tilde{M} . For the case of two orthogonal fiber modes linearly polarized along the x and y directions, the collection efficiency is expressible as an incoherent sum of the contribution from each fiber polarization mode $\eta = \eta^x + \eta^y$. The result is plotted in Fig. 2(a), showing that the maximum collection efficiency is obtained when $\tilde{M}=f_3/f_1=6.75$ (corresponding to a magnification of $M=8.97$). At this focal length ratio, we calculate a coupling efficiency of approximately 51%. Finally, for comparison, we assume NA₃=0.13 for the single-mode fiber and use the relationship $NA_1/(n_1NA_3)=\tilde{M}$ to find $\tilde{M}=6.95$. Comparing the value $\tilde{M}=6.95$ with Fig. 2(a) reveals the refractive index-scaled numerical aperture ratio results in a focal length ratio that nearly maximizes the collection efficiency as determined by evaluating Eq. (4). We find this simple rule to be generally valid by comparing the evaluation of Eq. (4) as a function of \tilde{M} with $NA_1/(n_1NA_3)=\tilde{M}$, varying the numerical aperture of the collection objective from NA₁=0.4 to 1.2.

Next, fixing $\tilde{M}=6.75$ we calculate the collection efficiency $\eta(\rho_o=x, \phi_o=0, z_o=z; \tilde{M}=6.75)$ when the dipole is displaced in the object space. The results are presented in Fig. 2(b). Figure 2(c) [Fig. 2(d)] presents the transverse (axial) resolution, defined by the Houston criteria, calculated by evaluating the full width at half-maximum of the collection efficiency $\eta(\rho_o=0, \phi_o=0, z_o=z; \tilde{M})$ [$\eta(\rho_o=0, \phi_o=0, z_o=z; \tilde{M})$] when the dipole is displaced along the x (z) direction in the object space. With $\tilde{M}=6.75$ (the focal length ratio of maximum light collection), we calculate a transverse resolution of 0.525λ and an axial resolution of 1.65λ . We find that the maximum of collection efficiency does not coincide with the microscope's diffraction-limited resolution.

In summary, we find for fixed collection objective numerical aperture and single-mode fiber characteristics, there is a particular value of the objective focal length ratio \tilde{M} that maximizes the collection efficiency η . However, Fig. 2 makes clear that in constructing a fiber-based confocal microscope there is a compromise between instrument collection efficiency and optical resolution. It is important in system design to determine which figure of merit, collection efficiency or resolution, is most important.

This work was supported by Air Force Office of Scientific Research under grant MURI F-49620-03-1-0379, by National Science Foundation under grant NIRT ECS-0210752 and a Boston University SPRInG grant. The authors thank Lukas Novotny for many helpful discussions. A. Vamivakas's e-mail address is nvami@bu.edu.

References

1. L. Novotny and B. Hecht, *Principles of Nano-Optics*, 1st ed. (Cambridge U. Press, 2006).
2. S. Inoué, in *Handbook of Biological Confocal Microscopy*, 2nd ed., J. B. Pawley, ed. (Plenum, 1995), p. 1.
3. C. J. R. Sheppard and T. Wilson, Proc. R. Soc. London, Ser. A **379**, 145 (1982).
4. J. Enderlein, Opt. Lett. **25**, 634 (2000).
5. M. Gu, C. J. R. Sheppard, and X. Gan, J. Opt. Soc. Am. A **8**, 1755 (1991).
6. X. Gan, M. Gu, and C. J. R. Sheppard, J. Mod. Opt. **39**, 825 (1992).
7. M. Gu and C. J. R. Sheppard, J. Mod. Opt. **38**, 1621 (1991).
8. S. B. Ippolito, B. B. Goldberg, and M. S. Ünlü, J. Appl. Phys. **97**, 053105 (2005).
9. Z. Liu, B. B. Goldberg, S. B. Ippolito, A. N. Vamivakas, M. S. Ünlü, and R. P. Mirin, Appl. Phys. Lett. **87**, 071905 (2005).
10. A fiber-based confocal microscope is utilized by Liu⁹ to study individual quantum dots.
11. E. Wolf, Proc. R. Soc. London, Ser. A **253**, 349 (1959).
12. B. Richards and E. Wolf, Proc. R. Soc. London, Ser. A **253**, 358 (1959).
13. D. Glöge, Appl. Opt. **10**, 2252 (1971).
14. J. Buck, *Fundamentals of Optical Fibers*, 2nd ed. (Wiley, 2004).